

Electron-Phonon Coupling and the Soft Phonon Mode in TiSe₂

F. Weber,^{1,2,*} S. Rosenkranz,² J.-P. Castellan,² R. Osborn,² G. Karapetrov,² R. Hott,¹ R. Heid,¹ K.-P. Bohnen,¹ and A. Alatas³

¹Karlsruher Institut für Technologie, Institut für Festkörperphysik, P.O.B. 3640, D-76021 Karlsruhe, Germany

²Materials Science Division, Argonne National Laboratory, Argonne, Illinois, 60439, USA

³Advanced Photon Source, Argonne National Laboratory, Argonne, Illinois, 60439, USA

(Dated: May 29, 2018)

We report high-resolution inelastic x-ray measurements of the soft phonon mode in the charge-density-wave compound TiSe₂. We observe a complete softening of a transverse optic phonon at the L point, i.e. $\mathbf{q} = (0.5, 0, 0.5)$, at $T \approx T_{CDW}$. Renormalized phonon energies are observed over a large wavevector range $(0.3, 0, 0.5) \leq \mathbf{q} \leq (0.5, 0, 0.5)$. Detailed *ab-initio* calculations for the electronic and lattice dynamical properties of TiSe₂ are in quantitative agreement with experimental frequencies for the phonon branch involving the soft mode. The observed broad range of renormalized phonon frequencies is directly related to a broad peak in the electronic susceptibility stabilizing the charge-density-wave ordered state. Our analysis demonstrates that a conventional electron-phonon coupling mechanism can explain a structural instability and the charge-density-wave order in TiSe₂ although other mechanisms might further boost the transition temperature.

PACS numbers: 71.45.Lr, 63.20.kd, 63.20.dd, 63.20.dk

The origin of charge-density-wave (CDW) order, i.e., a periodic modulation of the electronic density, is a long-standing problem relevant to a number of important issues in condensed matter physics, such as the role of stripes in cuprates [1] and charge fluctuations in the colossal magnetoresistive manganites [2]. Chan and Heine derived the criterion for a stable CDW phase with a modulation wavevector \mathbf{q} as [3]

$$\frac{4\eta_q^2}{\hbar\omega_{bare}} \geq \frac{1}{\chi_q} + (2U_q - V_q) \quad (1)$$

where η_q is the electron-phonon coupling (EPC) matrix element associated with a mode at an unrenormalized energy of ω_{bare} , χ_q is the dielectric response of the conduction electrons, and U_q and V_q are their Coulomb and exchange interactions. Static CDW order typically is taken as a result of a divergent electronic susceptibility χ_q due to nesting, i.e. parallel sheets of the Fermi surface (FS) separated by twice the Fermi wavevector $2k_f$. Electron-phonon coupling (EPC) is required to stabilize the structural distortion and, hence, an acoustic phonon mode at the CDW wavevector $\mathbf{q}_{CDW} = 2k_f$ softens to zero energy at the transition temperature T_{CDW} [3, 4]. However, when electronic probes reported only small and not well nested Fermi surfaces this scenario has been discarded for the prototypical CDW compound TiSe₂ [5–7].

Alternative scenarios such as indirect or band-type Jahn-Teller effects [6–8] and, most prominently, exciton formation [5, 9, 10] are discussed in the theoretical as well as experimental literature. More recently, van Wezel et al. have invoked a model including exciton formation as well as EPC [11] and have shown that it can explain data from angle-resolved photoemission spectroscopy (ARPES) [12], formerly taken as evidence of an

excitonic insulating phase in TiSe₂ [9]. Determining the origin of CDW formation in TiSe₂ is all the more important with respect to the nature of superconductivity, which emerges both as function of pressure [13] and Cu intercalation [14]. In particular, pressure induced superconductivity is expected to be closely linked to the nature of the parent CDW state.

In this letter, we report a temperature dependent study of the CDW soft phonon mode in TiSe₂ by high-resolution inelastic x-ray (IXS) scattering. We investigated both phonon energies as well as the phonon linewidths. We observe a complete softening of a transverse phonon branch at the L point close to the CDW transition temperature T_{CDW} . Calculations of the lattice dynamical properties based on density-functional-perturbation theory (DFPT) describe our results very well and demonstrate that conventional EPC can stabilize CDW order contrary to the current discussion in the literature [7, 9, 11].

Our sample was a high-quality single crystal with dimensions $(3 \times 3 \times 0.05)$ mm³ that shows a sharp onset of a $(2 \times 2 \times 2)$ CDW superstructure at $T_{CDW} \approx 200$ K as observed by synchrotron x-ray diffraction (XRD) [15]. The high-resolution IXS experiments were carried out at the XOR 3-ID HERIX beamline of the Advanced Photon Source, Argonne National Laboratory. The incident energy was 21.657 keV and the horizontally scattered beam was analyzed by a spherically curved silicon analyser (Reflection [18, 6, 0]). The full width at half maximum (FWHM) of the energy and wavevector space resolution was 2.4 meV and 0.07 \AA^{-1} , respectively. The components (Q_h, Q_k, Q_l) of the scattering vector are expressed in reciprocal lattice units (r.l.u.) $(Q_h, Q_k, Q_l) = (h * 2\pi/a, k * 2\pi/a, l * 2\pi/c)$; with the lattice constants $a = 3.54 \text{ \AA}$ and $c = 6.01 \text{ \AA}$ of the hexag-

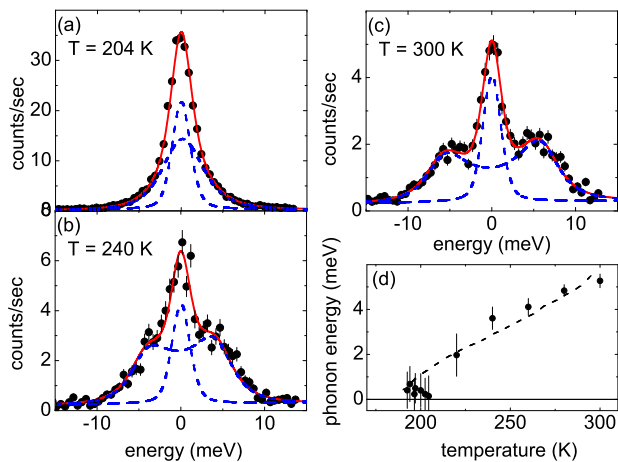


FIG. 1. (Color online) Temperature dependence of soft phonon mode at $\mathbf{Q} = (-0.5, 1, 0.5)$ (L point). (a)-(c) Energy scans for temperatures $204 \text{ K} \leq T \leq 300 \text{ K}$. Solid (red) lines are fits consisting of a damped harmonic oscillator (inelastic) and a pseudo-voigt function (elastic) (blue dashed lines). (d) Soft mode energy ω_q observed via IXS as function of temperature. The dashed line in (f) is the temperature dependence deduced from thermal diffuse scattering reproduced from Ref. 23.

onal unit cell ($P\bar{3}m1$, 164).

Measured energy spectra were fitted using a pseudo-Voigt function for the elastic line with a variable amplitude and fixed lineshape determined from scans through the CDW superlattice peak at base temperature. The phonon was fitted by a damped harmonic oscillator (DHO) function, where the energy ω_q of the damped phonon is given by $\omega_q = \sqrt{\tilde{\omega}_q^2 - \Gamma^2}$ [16], where $\tilde{\omega}_q$ is the phonon energy renormalized only by the real part of the susceptibility, and Γ denotes the phonon linewidth, which is closely related to the imaginary part of the susceptibility. The situation, where the phonon becomes overdamped and freezes into a periodic lattice distortion, is defined when the damping ratio $\Gamma/\tilde{\omega}_q$ reaches its critical value, $\Gamma/\tilde{\omega}_q = 1$.

Density-functional-theory calculations were performed in the framework of the mixed basis pseudopotential method [17]. The exchange-correlation functional was treated in the local-density approximation (LDA). Norm-conserving pseudo-potentials for Ti and Se were constructed with Ti 3s and 3p semicore states included in the valence space. Phonon frequencies and electronic contributions to the phonon linewidth were calculated using the linear response technique or density functional perturbation theory (DFPT) [18] in combination with the mixed-basis pseudopotential method [19]. To resolve fine features related to the Fermi surface geometry, Brillouin-zone (BZ) integrations were performed with a dense hexagonal $24 \times 24 \times 8$ k -point mesh (244 points in the ir-

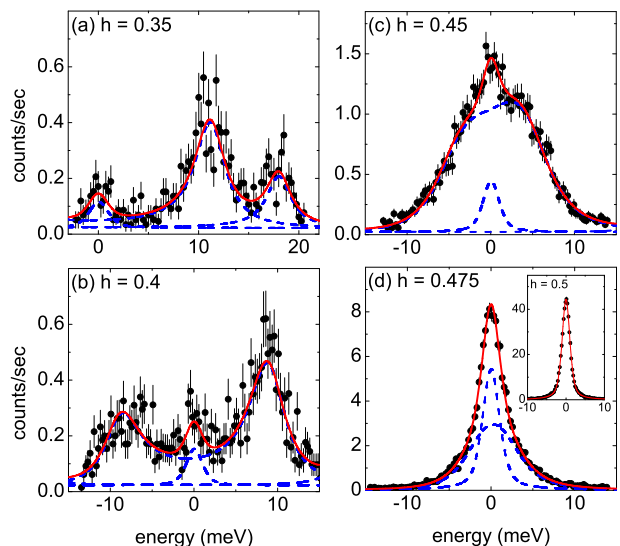


FIG. 2. (Color online) Energy scans at $\mathbf{Q} = (-h, 1, 0.5)$, $h = 0.35 - 0.5$, for temperature $T = 190 \text{ K}$ ($\approx T_{CDW}$). Solid lines represent the total fit result consisting of a damped harmonic oscillator for the inelastic and a pseudo-voigt function for the elastic scattering (blue dashed lines). The inset of (d) shows the scan at $h = 0.5$, which can be well described just by the pseudo-voigt as used in (a)-(d).

reducible BZ). The standard smearing technique was employed with a Gaussian broadening of $\sigma = 0.15 \text{ eV}$. Displayed results were obtained for the undistorted hexagonal structure using experimental lattice constants and optimized internal parameters. The calculated electronic structure and lattice dynamical properties are in good agreement with previous results from LDA [20, 21].

Fig. 1 shows the temperature dependence of the soft phonon mode measured at the L -point, i.e. $\mathbf{Q} = (-0.5, 1, 0.5)$, from temperatures just above T_{CDW} up to room temperature (Fig. 1a-c). At room temperature we find a phonon energy $\omega_q = 5.3 \text{ meV}$ in good agreement with previous neutron scattering data [22]. On lowering the temperature, ω_q softens to zero energy (within the experimental error) already at $T = 204 \text{ K}$. At $T_{CDW} \leq T \leq 204 \text{ K}$, the phonon is overdamped and can only be observed as a broad quasi-elastic peak underneath the sharp elastic line, which becomes gradually more dominant below 200 K (not shown). For $T \leq 190 \text{ K}$ low energy phonon scattering directly at the L point was undetectable due to the strong CDW superstructure peak. Overall, our results roughly agree with energies of the soft mode deduced from thermal diffuse scattering [23].

We studied in detail the dispersion of the transverse optic (TO) phonon starting at 17 meV at A and ending in the CDW related soft mode at L , i.e. $\mathbf{q} = (-h, 0, 0.5)$ and $0 \leq h \leq 0.475$ [?]. We note that at $h \approx 0.33$ there is an anti-crossing of this TO branch with an acoustic-

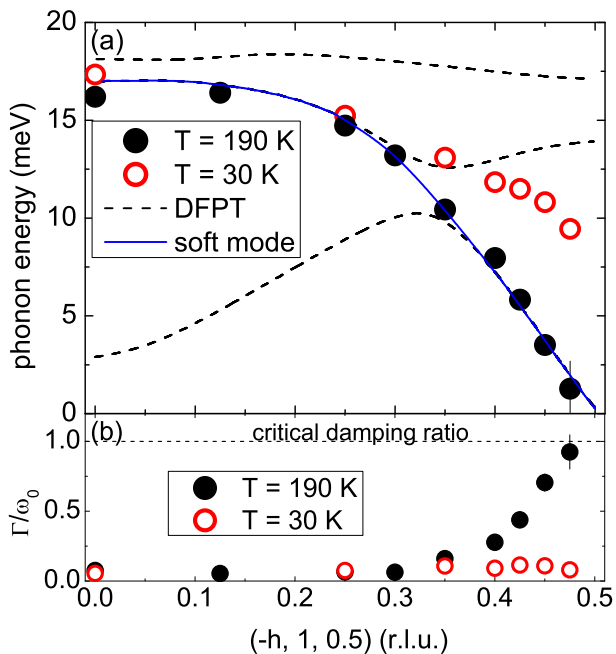


FIG. 3. (Color online) (a) Dispersion of the soft phonon mode at $T = 190$ K ($\approx T_{CDW}$, filled symbols) and $T = 30$ K (open circles) along $\mathbf{Q} = (-h, 1, 0.5)$, $h = 0-0.475$. Dashed lines are results of DFPT calculations using the experimental crystal structure and $\sigma = 0.15$ eV. The solid (blue) line indicates the dispersion of the soft mode character across the anti-crossing at $h \approx 0.33$. Frequencies of the upward dispersing branch (e.g. see fig. 2(a)) agree well with the calculation but are not shown for the sake of clarity. (b) Damping ratio of the DHO at $T = 190$ K (filled symbols) and $T = 30$ K (open circles).

like upward dispersing branch. The character of the soft mode is transferred to the energetically lower branch for $h > 0.33$. For simplicity, we speak of the soft-mode dispersion as represented by the dashed (blue) line in Fig. 3a, which involves parts of the TO branch ($h < 0.33$) and the acoustic-like branch ($h > 0.33$). A set of energy scans taken at $T = 190$ K is shown in Fig. 2.

At $h = 0.35$ (Fig. 2a), we observe two phonon peaks, where the one at lower energies corresponds to the character of the soft mode starting at 17 meV at A . The second peak near 17 meV represents the continuation of the upward dispersing acoustic-like branch in good agreement with structure factor calculations by DFPT. This mode does not show any significant temperature dependence. Results of its dispersion are not shown in Fig. 3 for the sake of clarity and will be discussed in detail elsewhere.

The energy of the phonon peak related to the soft mode already decreases for $h \geq 0.25$ and, after the anti-crossing, shows a quasi-linear dispersion relation for $h \geq 0.4$ (Fig. 2b-d), which extrapolates to a zero phonon energy at $h = 0.5$ (Fig. 3a). At $h = 0.5$ however, the strong CDW superlattice reflection made it impossible

to directly measure the quasielastic scattering expected for the critically damped phonon. The calculated dispersions agree very well with these results. Corresponding to the strong renormalization of the phonon energy, we observe an increase of the damping ratio Γ/ω_q , which stays just below 1 for $h = 0.475$. But just like the energy, the damping ratio also shows linear behavior for $h \geq 0.4$ and extrapolates to an overdamped phonon at $h = 0.5$ (Fig. 3b).

The range in \mathbf{q} over which phonon energies are renormalized as function of temperature allows us to infer how sharp corresponding electronic signatures, e.g. in χ_q in a nesting scenario, might be [4]. We note that, in principle, the \mathbf{q} dependence of the EPC matrix element η_q can determine the periodicity of the low temperature superstructure as well [24]. Because the soft mode at $T = 300$ K is still far from being unrenormalized ($\Gamma/\omega_q(T = 300 \text{ K}) = 0.5$), we compare the dispersion at $T = 190$ K with results for $T = 30$ K in the CDW ordered state, as the latter give a good idea of the range of renormalized phonons. Fig. 3 clearly shows, that the phonon energies over the range $0.3 \leq h \leq 0.5$ are renormalized across the CDW transition. This large range in h is in contrast to compounds, where a sharp FS nesting drives the CDW formation and renormalized phonon energies are observed only over a much smaller \mathbf{q} range [25, 26].

Comparing the experimental results in more detail to the calculations, it is important to note that DFPT is a single particle response theory and, therefore, cannot include, e.g., exciton formation. However, EPC is calculated in great detail and, in particular, the electronic contribution to the phonon linewidth 2γ can be deduced (Fig. 4). 2γ of a specific phonon mode in turn can be approximately expressed as [27]

$$2\gamma = 4\pi\omega_{bare} \times |\eta_q|^2 \times JDOS \quad (2)$$

where the electronic joint density-of-states ($JDOS$) in turn is closely related to the imaginary part of the electronic susceptibility χ_q . We see that the \mathbf{q} range over which 2γ shows a strong enhancement matches closely the range of observed renormalized phonon energies (Fig. 3a). Furthermore, 2γ also qualitatively explains the \mathbf{q} dependence of the observed linewidth Γ very well (see Fig. 4b). Quantitatively, the calculated linewidth is a factor of 2.5 smaller than observed in experiment. Here, we note that similar observations have been made in the CDW compound NbSe₂ [24] and the conventional superconductor YNi₂B₂C [28]. In the latter, it is evident that only the lowest acoustic modes, which exhibit strong EPC, show this effect of too small calculated linewidths, whereas the linewidths of higher energy modes are predicted in much better agreement [29]. Therefore, we think that soft modes as in TiSe₂ are subject to an increased anharmonicity close to the structural phase transition reflected in an increased linewidth, which is not captured in our theory.

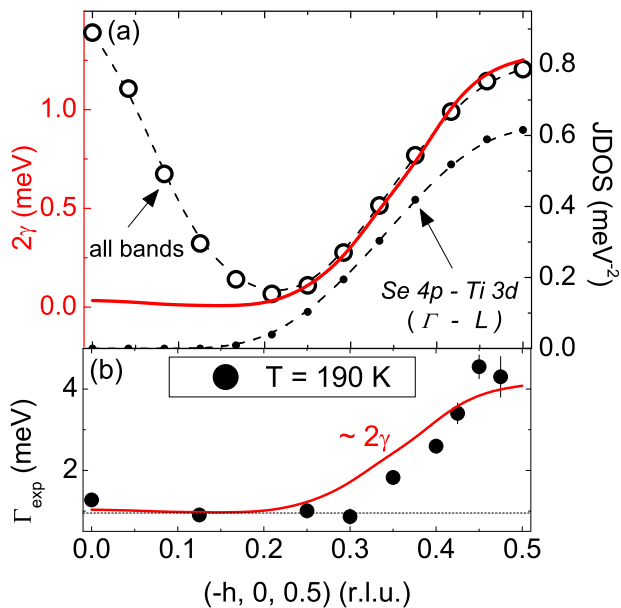


FIG. 4. (Color online) (a) Results of the calculation are shown as function of h along the $A-L$ line, i.e. $\mathbf{q} = (h, 0, 0.5)$ with $h = 0 - 0.5$: (1) the calculated electronic contribution to the phonon linewidth 2γ of the soft phonon mode (FWHM, solid line, left hand scale), (2) the total electronic $JDOS$ (open symbols, right-hand scale) and (3) interband contributions to the $JDOS$ between the Se 4p and Ti 3d bands near Γ and L (filled symbols, right-hand scale). (b) Experimental linewidth Γ (dots) compared to scaled 2γ ($\times 2.5 + \text{offset}$, solid line).

We now discuss the different contributions to 2γ , i.e. $|\eta_q|$ and the $JDOS$, according to equ. 2. The fact that 2γ for the soft phonon does not follow the increase of the total $JDOS$ below $h = 0.2$ is due to the presence of different bands near the Fermi energy. Whereas the $JDOS$ at small h is dominated by scattering processes within the Se 4p bands around the Γ point, at large h scattering between Se 4p and Ti 3d bands dominate (Fig. 4a). Apparently, η_q of the soft mode only samples the latter scattering processes. Using equation 2, $\omega_{bare} = 17$ meV and the partial $JDOS$ of Se 4p - Ti 3d scattering processes, we can calculate $|\eta_q|$. However, this is only possible for $h \geq 0.25$ as scattering processes of the same type seem to contribute to the EPC of different phonon modes for $h < 0.25$ and a clear determination of the relevant $JDOS$ is not possible anymore. We calculate $|\eta_q| = 0.098$ meV at $h = 0.5$ and a 33% decrease towards $h = 0.25$. For the same \mathbf{q} range, the partial $JDOS$ of Se 4p - Ti 3d scattering processes decreases by a factor of six. Hence, the \mathbf{q} dependence of the $JDOS$ is the dominant factor in the large increase of the phonon linewidth. The corresponding phonon renormalization then leads to the structural instability at the L point.

Our results explain the CDW phase transition in TiSe₂ in the conventional picture of an increased electronic sus-

ceptibility at \mathbf{q}_{CDW} aided by a strong EPC matrix element. This is not in contradiction to ARPES data, on the basis of which FS nesting previously has been ruled out as a driving force of the CDW transition in TiSe₂ [7]. Indeed, our results confirm that TiSe₂ does not exhibit a divergent $JDOS$. However, the peak in the $JDOS$ is connected with an enhancement of $Re \chi$ [21], which can, according to equ. 1, tip the balance between undistorted and CDW ordered phases if stabilized by a sufficiently large η_q . We note that DFPT is a zero temperature approach and, therefore, cannot calculate a transition temperature corresponding to, e.g., the calculated EPC strength. So, EPC might be only one ingredient for driving the CDW transition in TiSe₂, but our analysis shows that its importance has been greatly underestimated.

In conclusion we have reported a detailed analysis of the soft phonon behaviour in the CDW compound TiSe₂. The experimental observations are well reproduced by ab-initio calculations, which demonstrate that electron-phonon-coupling is strong enough to stabilize a structural phase transition in TiSe₂ at finite temperatures. Our work emphasizes the essential part of electron-phonon coupling matrix elements and provides a new route to seemingly mysterious phase transitions as far as the electronic footprint is concerned.

We acknowledge valuable discussions with Jasper van Wezel and Mike Norman. Work at Argonne was supported by U.S. Department of Energy, Office of Science, Office of Basic Energy Sciences, under contract No. DE-AC02-06CH11357.

* frank.weber@kit.edu

- [1] S. A. Kivelson, I. P. Bindloss, E. Fradkin, V. Oganesyan, J. M. Tranquada, A. Kapitulnik, and C. Howald, *Rev. Mod. Phys.* **75**, 1201 (2003)
- [2] E. Dagotto, *Science* **309**, 257 (2005)
- [3] S. K. Chan and V. Heine, *J. Phys. F: Metal Phys.* **3**, 795 (1973)
- [4] G. Grüner, *Rev. Mod. Phys.* **60**, 1129 (1988)
- [5] J. A. Wilson, *Solid State Commun.* **22**, 551 (1977)
- [6] H. P. Hughes, *J. Phys. C: Solide State Phys.* **10**, L319 (1977)
- [7] K. Rossnagel, L. Kipp, and M. Skibowski, *Phys. Rev. B* **65**, 235101 (2002)
- [8] M. Whangbo and E. Canadell, *J. Amer. Chem. Soc.* **114**, 9587 (1992)
- [9] H. Cercellier, C. Monney, F. Clerc, C. Battaglia, L. Despont, M. G. Garnier, H. Beck, P. Aebi, L. Patthey, H. Berger, and L. Forró, *Phys. Rev. Lett.* **99**, 146403 (2007)
- [10] T. Rohwer, S. Hellmann, M. Wiesenmayer, C. Sohr, A. Stange, B. Slomski, A. Carr, Y. Liu, L. M. Avila, M. Kallane, S. Mathias, L. Kipp, K. Rossnagel, and M. Bauer, *Nature* **471**, 7339 (2011)
- [11] J. van Wezel, P. Nahai-Williamson, and S. S. Saxena, *Phys. Rev. B* **81**, 165109 (2010)
- [12] J. van Wezel, P. Nahai-Williamson, and S. S. Saxena,

- Europhys. Lett.* **89**, 47004 (2010)
- [13] A. Kusmartseva, B. Sipos, H. Berger, L. Forró, and E. Tutiš, *Phys. Rev. Lett.* **103**, 236401 (2009)
- [14] E. Morosan, H. W. Zandbergen, B. S. Dennis, J. W. G. Bos, Y. Onose, T. Klimczuk, A. P. Ramirez, N. P. Ong, and R. J. Cava, *Nature Physics* **2**, 544 (2006)
- [15] S. Rosenkranz, J. P. Castellán, F. Weber, R. Osborn, and G. Karapetrov, *unpublished*
- [16] G. Shirane, S. Shapiro, and J. Tranquada, *Neutron Scattering with a Triple-Axis Spectrometer*, Cambridge University Press (2002)
- [17] B. Meyer, C. Elssser, F. Lechermann, and M. Föhnle, *Max-Planck-Institut für Metallforschung, Stuttgart*
- [18] S. Baroni, S. de Gironcoli, A. Dal Corso, and P. Gianozzi, *Rev. Mod. Phys.* **73**, 515 (2001)
- [19] R. Heid and K.-P. Bohnen, *Phys. Rev. B* **60**, R3709 (1999)
- [20] R. A. Jishi and H. M. Alyahyaei, *Phys. Rev. B* **78**, 144516 (2008)
- [21] M. Calandra and F. Mauri, *Phys. Rev. Lett.* **106**, 196406 (2011)
- [22] N. Wakabayashi and H. G. Smith, *Solid State Commun.* **28**, 923 (1978)
- [23] M. Holt, P. Zschack, H. Hong, M. Y. Chou, and T.-C. Chiang, *Phys. Rev. Lett.* **86**, 3799 (2001)
- [24] F. Weber, S. Rosenkranz, J. P. Castellán, R. Osborn, R. Hott, R. Heid, K.-P. Bohnen, T. Egami, A. H. Said, and D. Reznik, *Phys. Rev. Lett.* **107**, 107403 (2011)
- [25] B. Renker, H. Rietschel, L. Pintschovius, W. Gläser, P. Brüesch, D. Kuse, and M. J. Rice, *Phys. Rev. Lett.* **30**, 1144 (1973)
- [26] M. Hoesch, A. Bosak, D. Chernyshov, H. Berger, and M. Krisch, *Phys. Rev. Lett.* **102**, 086402 (2009)
- [27] R. Heid, K.-P. Bohnen and Renker, *Adv. Solid State Phys.* **42**, 293 (2002)
- [28] L. Pintschovius, F. Weber, W. Reichardt, A. Kreyssig, R. Heid, D. Reznik, O. Stockert and K. Hradil, *Pramana - journal of physics* **71**, 687 (2008)
- [29] F. Weber, S. Rosenkranz, L. Pintschovius, J.-P. Castellán, R. Osborn, W. Reichardt, R. Heid, K.-P. Bohnen, E. Goremychkin and D. Abernathy, *unpublished*